

Mesoporous Carbon Single-Crystals from Organic–Organic Self-Assembly

Fuqiang Zhang, Dong Gu, Ting Yu, Fan Zhang, Songhai Xie, Lijuan Zhang, Yonghui Deng, Ying Wan, Bo Tu, and Dongyuan Zhao*

Department of Chemistry, Shanghai Key Laboratory of Molecular Catalysis and Innovative Materials, Fudan University, Shanghai 200433, P. R. China

Received April 2, 2007; E-mail: dyzhao@fudan.edu.cn

A single-crystal is a solid in which the atoms and molecules are periodically stacked by chemical bonds across its whole volume. The special repeating manner offers good opportunities to understand the growth mechanism of crystals and find important applications in integrated circuits, optic devices, etc. Mesoporous silica single-crystals, although well-known in the form of amorphous silica, have mesoscopic periodic regularity.¹ It is quite different from atomic single-crystals in which each atom is related to every equivalent atom in the structure by translational symmetry. Mesoporous single-crystals with perfect long-range ordering in mesoscale also facilitate the structural resolution and understanding of the formation of mesostructures² and have great potential applications as nanodevices based on crystallization on the mesoscale. A variety of mesoporous silica single-crystals with 3-D cubic or hexagonal structures have emerged.^{1–6} The syntheses were achieved by the surfactant-templating inorganic–organic self-assembly strategy under aqueous conditions.

Carbons with common crystalline forms of diamond, graphite, and fullerene are of great importance, because of their remarkable properties. Ordered mesoporous carbons have evoked enormous researches owing to their great potential applications in catalysis, separation, electrochemical double-layer capacitors, fuel cells, batteries, etc.^{7–13} Such materials were first demonstrated by employing a nanocasting strategy.⁷ The obtained ordered mesoporous carbons have the reverse mesostructures with the same symmetries as mesoporous silica. To date, a variety of mesoporous carbon materials have been successfully obtained from this strategy.^{7–9} However, during the fussy nanocasting procedures, numerous defects and large shrinkage were generated and aggrandized. In addition, the small entrance of 3-D cubic caged mesoporous silica may also inhibit the infiltration of carbon precursors. As a result, the replication of mesoporous carbon single-crystals is still difficult. Recently, we reported a one-step aqueous route to synthesize mesoporous carbon materials.¹³ This organic–organic self-assembly strategy results in the formation of a variety of mesoporous carbon, such as FDU-14 (*Ia3d*), FDU-15 (*p6mm*), and FDU-16 (*Im3m*). The aqueous route is an industrially feasible method for preparing highly ordered mesoporous carbons in large quantity. Nevertheless, the formation mechanism is not well understood.

In this paper, we report, for the first time, the synthesis of 3-D cubic mesoporous carbon FDU-16 single-crystals of rhombododecahedron with the uniform size of $\sim 5 \mu\text{m}$ by an aqueous organic–organic assembly of triblock copolymer F127 and phenol/formaldehyde resols. SEM and TEM images directly show a layer-by-layer growth mode of body-centered cubic FDU-16 single-crystals from the centers of twelve $\{110\}$ planes.

Mesoporous carbon FDU-16 (*Im3m*) with rhombododecahedral morphology was synthesized by an aqueous organic–organic assembly under a base condition with the com-

ponent molar ratio of F127/phenol/HCHO/NaOH/H₂O equal to 0.044:2.1:10:0.50:580. The small-angle X-ray scattering (SAXS) pattern (Supporting Information Figure SI 1A) of single-crystal mesoporous carbon FDU-16 shows a highly ordered cubic mesostructure of *Im3m* symmetry with a lattice size of 11.5 nm. The SEM image (Figure 1A) reveals that the calcined mesoporous carbon FDU-16 sample is composed of $\sim 100\%$ single-crystals of $\sim 5 \mu\text{m}$ with rhombododecahedral morphology. High-resolution FE-SEM images (Figure 1B) show that the perfect rhombododecahedron carbon crystals have a symmetry with three 4-fold axes and four 3-fold axes, commensurate with the *m3m* point group. The twelve equivalent faces can be indexed as the $\{110\}$ planes, which have the highest plane density and the lowest surface energy during the growth of crystals accordingly, as shown in a structural model (Figure 1C). High magnification FE-SEM image (Figure SI 2) further reveals the thin platelike layer structures in different levels that may reflect the trace of the crystal growth. A layer-by-layer growth of crystals from the centers of twelve $\{110\}$ planes can be clearly established. Several layers can grow simultaneously on one face of $\{110\}$ planes, and the terrace-like morphology is formed on each plane (Figure SI 3).

TEM images of mesoporous carbon FDU-16 single-crystals are shown in Figure 2 (Figure SI 4 of higher magnification), viewed along $[110]$ and $[100]$ directions. The crystals exhibit the same morphology with 3-D repetition of a body-centered cubic packing pattern as predicted from the structure models viewed along each direction (insets of Figure 2). The periodicity of the pattern extends throughout the whole material. No other type of patterns can be observed in the other area of the crystals. These observations confirm that the obtained mesoporous carbons with rhombododecahedron morphology are single crystals. It is worthy to note here that the layered structure can be directly observed viewed along the $[100]$ directions. Moreover, the thickness of each layer is ~ 8.0 nm, which is the same as the d_{110} -spacing value estimated from TEM images. It gives further evidence of the growth of carbon single-crystals via a layer-by-layer way from twelve $\{110\}$ planes (Figure SI 3), which is similar to that of mesoporous silica SBA-16 with the same symmetry,¹⁴ indicating a relating underlying driving force for the formation of mesostructured crystals with different composition.

The hexagonal mesoporous carbon FDU-15 with discuslike morphology can be obtained by using P123 and F127 as mixed templates. The SAXS pattern (Figure SI 1B) of calcined FDU-15 reveals ordered 2-D hexagonal *p6mm* structure with a lattice size of 9.4 nm. The SEM image shows that the mesoporous carbon FDU-15 has a uniform discuslike morphology with the size between 0.5 and $1 \mu\text{m}$ (Figure SI 5). The close-packed mesochannels can be directly seen on the external surface of FDU-15 as shown in the FE-SEM images with high magnification (Figure 1D,E). All channels of FDU-15 grow along the circumference of the discus.

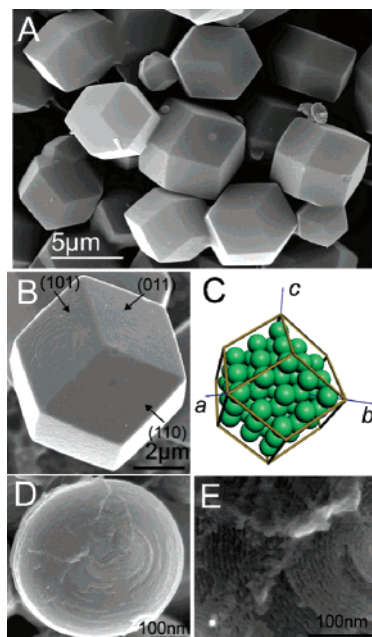


Figure 1. SEM images of calcined FDU-16 (A, B) and FDU-15 (D, E); structural model of FDU-16 (C).

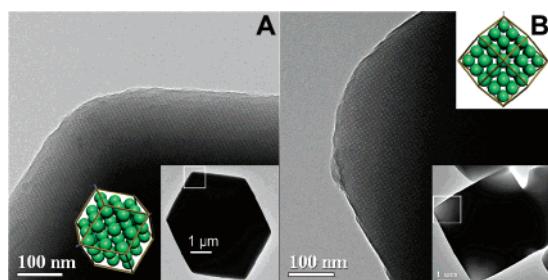


Figure 2. TEM image of FDU-16 single crystals viewed along [110] (A) and [100] (B) directions. Insets are the images of low magnification and structural models. The rectangle in each inset shows from where the corresponding large image was taken.

N_2 sorption isotherms (Figure SI 6) of mesoporous carbon FDU-16 and FDU-15 show type-IV curves with clear condensation steps, indicating uniform mesopores. Mesoporous carbon FDU-16 has a pore diameter of 2.8 nm calculated based on the KJS (Kruk–Jaroniec–Sayari) model,¹⁵ a pore volume of 0.38 cm³/g and a BET surface area of ~750 m²/g. FDU-15 possesses a mesopore diameter of 2.6 nm, a pore volume of 0.40 cm³/g, and a surface area of ~800 m²/g.

Our results show that both the stirring rate and synthesis temperature are key factors for the formation of high-quality FDU-16 single-crystals. The optimal rate is controlled at ~300 rpm, and the reaction temperature is close to 66 °C. A higher stirring rate (~500 rpm) could result in irregular morphology, while small crystals (1–2 μm) were obtained at a lower rate (~150 rpm). No precipitation could be observed at a temperature of ~70 °C, and only irregular crystals were obtained at ~60 °C.

The fabrication of mesoporous carbon single-crystals involves the building of a crystal layer by layer in mesoscale. The growth of crystals is limited by either the growing rate determined by the cross-link and polymerization of phenol resols or the assembly between resols and the triblock copolymer templates. It should be noted that both of them are in mesoscale, different from atomic crystals. The extremely low growing rate and strong hydrogen bonding¹⁶ between resols and the PEO segments of the copolymers favor the growth of mesostructured large single-crystals. Under the

present aqueous condition, it takes about 48 h to get the precipitation of crystals. The low stirring rate (~300 rpm) leads to suitable mass transport and slow growth rate, favoring the formation of large crystals. However, a too slow rate (~150 rpm) would bring about small crystals, implying a determined step of mesoscale mass transportation for controlling crystal growth, which is quite different from that for atomic crystals. The temperature can directly influence the polymerization of the resols and the hydrogen-bond interaction. With the increase of temperature, the hydrogen-bond interaction between the resols and the triblock copolymer templates is weakened and the polymerization of resols is accelerated. A medium temperature is adopted to balance the assembly and polymerization.

In summary, ordered cubic mesoporous carbon single-crystals with perfect rhombododecahedral morphology (FDU-16, *Im3m*) have been successfully synthesized by employing the organic–organic self-assembly of triblock copolymer and phenol/formaldehyde resols. A layer-by-layer growth mechanism of the mesoporous carbon single-crystals is directly demonstrated by the SEM and TEM images. 2-D hexagonal mesoporous carbon FDU-15 crystals with discuslike morphology have also been fabricated by mixing F127 with P123 as templates. These materials not only provide specification of crystal growth and mesostructure, but also will meet the demands of emerging nanodevice technologies.

Acknowledgment. This work was supported by NSFC (20421303, 20521140450), State Key Basic Research Program of PRC (2006CB202502, 2006CB0N0302), Shanghai Sci. & Tech. Committee (06DJ14006, 055207078, 05DZ22313), Shanghai Nanotech Promotion Center, Shanghai Education Committee, and New Century Excellent Talents. We thank Prof. P. Wu, L. Chen, H. Chen, and Y. Chen for characterization helps.

Supporting Information Available: Synthesis detail, SAXS patterns, SEM, TEM images, growing mechanism scheme, and nitrogen sorption isotherms of FDU-15 and FDU-16. This material is available free of charge via the Internet at <http://pubs.acs.org>.

References

- (1) Kim, J. M.; Kim, S. K.; Ryoo, R. *Chem. Commun.* **1998**, 259–260.
- (2) Kaneda, M.; Tsubakiyama, T.; Carlsson, A.; Sakamoto, Y.; Ohsuna, T.; Terasaki, O.; Joo, S. H.; Ryoo, R. *J. Phys. Chem. B* **2002**, *106*, 1256–1266.
- (3) Guan, S.; Inagaki, S.; Ohsuna, T.; Terasaki, O. *J. Am. Chem. Soc.* **2000**, *122*, 5660–5661.
- (4) (a) Che, S.; Kamiya, S.; Terasaki, O.; Tatsumi, T. *J. Am. Chem. Soc.* **2001**, *123*, 12089–12090. (b) Che, S.; Sakamoto, Y.; Terasaki, O.; Tatsumi, T. *Chem. Mater.* **2001**, *13*, 2237–2239.
- (5) Sayari, A.; Hamoudi, S.; Yang, Y.; Moudrakovski, I. L.; Ripmeester, J. R. *Chem. Mater.* **2000**, *12*, 3857–3863.
- (6) Yu, C. Z.; Tian, B. Z.; Fan, J.; Stucky, G. D.; Zhao, D. Y. *J. Am. Chem. Soc.* **2002**, *124*, 4556–4557.
- (7) Ryoo, R.; Joo, S. H.; Jun, S. J. *J. Phys. Chem. B* **1999**, *103*, 7743–7746.
- (8) Lu, A. H.; Schuth, F. *Adv. Mater.* **2006**, *18*, 1793–1805.
- (9) Lee, J.; Kim, J.; Hyeon, T. *Adv. Mater.* **2006**, *18*, 2073–2094.
- (10) Liang, C. D.; Hong, K. L.; Guiochon, G. A.; Mays, J. W.; Dai, S. *Angew. Chem., Int. Ed.* **2004**, *43*, 5785–5789.
- (11) Tanaka, S.; Nishiyama, N.; Egashira, Y.; Ueyama, K. *Chem. Commun.* **2005**, 2125–2127.
- (12) Meng, Y.; Gu, D.; Zhang, F. Q.; Shi, Y. F.; Yang, H. F.; Li, Z.; Yu, C. Z.; Tu, B.; Zhao, D. Y. *Angew. Chem., Int. Ed.* **2005**, *44*, 7053–7059.
- (13) (a) Zhang, F. Q.; Meng, Y.; Gu, D.; Yan, Y.; Yu, C. Z.; Tu, B.; Zhao, D. Y. *J. Am. Chem. Soc.* **2005**, *127*, 13508–13509. (b) Zhang, F. Q.; Meng, Y.; Gu, D.; Yan, Y.; Chen, Z. X.; Tu, B.; Zhao, D. Y. *Chem. Mater.* **2006**, *18*, 5279–5288.
- (14) Terasaki, O.; Ohsuna, T.; Liu, Z.; Sakamoto, Y.; Garcia-Bennett, A. E. In *Mesoporous Crystals and Related Nano-Structured Materials*; Elsevier Science BV: Amsterdam, 2004; Vol. 148, pp 261–288.
- (15) Kruk, M.; Jaroniec, M.; Sayari, A. *Langmuir* **1997**, *13*, 6267–6273.
- (16) Chu, P. P.; Wu, H. D. *Polymer* **2000**, *41*, 101–109.

JA072316D